environmental microbiology

Environmental Microbiology (2018) **20**(2), 632–644 doi:10.1111/1462-2920.13986

Metaproteomics reveals major microbial players and their metabolic activities during the blooming period of a marine dinoflagellate *Prorocentrum donghaiense*

Dong-Xu Li,[1] Hao Zhang,[1] Xiao-Huang Chen,[1] Zhang-Xian Xie,[1] Yong Zhang,[1] Shu-Feng Zhang,[1] Lin Lin,[1] Feng Chen[2] and Da-Zhi Wang[1]*

[1]*State Key Laboratory of Marine Environmental Science/College of the Environment and Ecology, Xiamen University, Xiamen, China.*

[2]*Institute of Marine and Environmental Technology, University of Maryland Center for Environmental Science, Baltimore, MD, USA.*

Summary

Interactions between bacteria and phytoplankton during bloom events are essential for both partners, which impacts their physiology, alters ambient chemistry and shapes ecosystem diversity. Here, we investigated the community structure and metabolic activities of free-living bacterioplankton in different blooming phases of a dinoflagellate *Prorocentrum donghaiense* using a metaproteomic approach. The *Fibrobacteres-Chlorobi-Bacteroidetes* group, *Rhodobacteraceae*, SAR11 and SAR86 clades contributed largely to the bacterial community in the middle-blooming phase while the *Pseudoalteromonadaceae* exclusively dominated in the late-blooming phase. Transporters and membrane proteins, especially TonB-dependent receptors were highly abundant in both blooming phases. Proteins involved in carbon metabolism, energy metabolism and stress response were frequently detected in the middle-blooming phase while proteins participating in proteolysis and central carbon metabolism were abundant in the late-blooming phase. Beta-glucosidase with putative algicidal capability was identified from the *Pseudoalteromonadaceae* only in the late-blooming phase, suggesting an active role of this group in lysing *P. donghaiense* cells. Our results indicated that diverse substrate utilization strategies and different capabilities for environmental adaptation among bacteria shaped their distinct niches in different bloom phases, and certain bacterial species from the *Pseudoalteromonadaceae* might be crucial for the termination of a dinoflagellate bloom.

Received 6 June, 2017; revised 12 September, 2017; accepted 27 October, 2017. *For correspondence. E-mail dzwang@xmu.edu.cn; Tel. (+86) 592 2186016; Fax (+86) 592 2180655.

Introduction

Phytoplankton blooms are a seasonal event in the ocean that is of crucial importance for nutrient cycling and ecosystem function (Kirchman *et al.*, 1991). Recent studies show that a phytoplankton bloom can trigger a succession of microbial predators and scavengers (Amin *et al.*, 2012; Buchan *et al.*, 2014). During the phytoplankton bloom, some bacteria are closely related to the bloom-forming phytoplankton species and exhibit significant effects on these species and their production (Needham and Fuhrman, 2016; Teeling *et al.*, 2016). A large number of phytoplankton substrates, particularly dissolved organic carbon, are absorbed by bacteria for their growth (Kirchman *et al.*, 1991; Amon and Benner, 1996), and some bacterial species, such as *Flavobacteriia*, *Alphaproteobacteria* and *Gammaproteobacteria* can proliferate rapidly during a phytoplankton bloom (Larsen *et al.*, 2004; Niu *et al.*, 2011; Tada *et al.*, 2011; Teeling *et al.*, 2012; Tan *et al.*, 2015; Needham and Fuhrman, 2016). Conversely, bacteria can remineralize complex organic matter to produce inorganic nutrients for phytoplankton growth, or secrete algicidal compounds to kill the phytoplankton (Mayali and Azam, 2004; Liu *et al.*, 2008). Certain bacterial populations may be crucial for blooming dynamics and succession (Buchan *et al.*, 2014). Thus, exploration of bacterial population dynamics and functions during phytoplankton blooms is essential for understanding the relationships between bacteria and phytoplankton.

Diatoms and dinoflagellates are the two major causative organisms responsible for coastal phytoplankton blooms around the world, which impact ecosystem structure and function (Anderson *et al.*, 2012). Studies show that a diatom bloom induces a dynamic succession of bacterioplankton populations, and diatom-originated substrates control the succession (Teeling *et al.*, 2012; Teeling *et al.*, 2016). However, little is known about bacterial response to

© 2017 Society for Applied Microbiology and John Wiley & Sons Ltd

natural dinoflagellate blooms although variations of bacterial communities are witnessed in laboratory culture (Kodama *et al.*, 2006). Considering the vast physiological and genetic differences between dinoflagellates and diatoms (Smayda, 2002), it is, therefore, necessary to study bacterioplankton dynamics and metabolic activity during dinoflagellate blooms to further our understanding of dinoflagellate-bacteria interactions.

The dinoflagellate *Prorocentrum donghaiense* is a major causative agent of harmful algal blooms along the coast of China, which result in serious damage to the ecosystem and mariculture (Zhou *et al.*, 2003). Much effort has been devoted to the physiological ecology of *P. donghaiense* blooms (Zhou *et al.*, 2003; Zhou, 2010; Zhou *et al.*, 2017). However, very little is known about microbial community dynamics and their metabolic activities during the bloom period. In this study, we investigated community structure and protein expression profiles of free-living bacterioplankton during the blooming period of *P. donghaiense* along the coast of the East China Sea (Fig. 1) using a metaproteomic approach combined with 16S rRNA gene sequencing. We focussed on the blooming phase owing to the high metabolic activity of blooming cells. Major bacterial groups and their metabolic activities differed significantly in the middle- and late-blooming phases. Our results provided insights into the interaction mechanism between bloom-forming cells and bacteria during a dinoflagellate bloom.

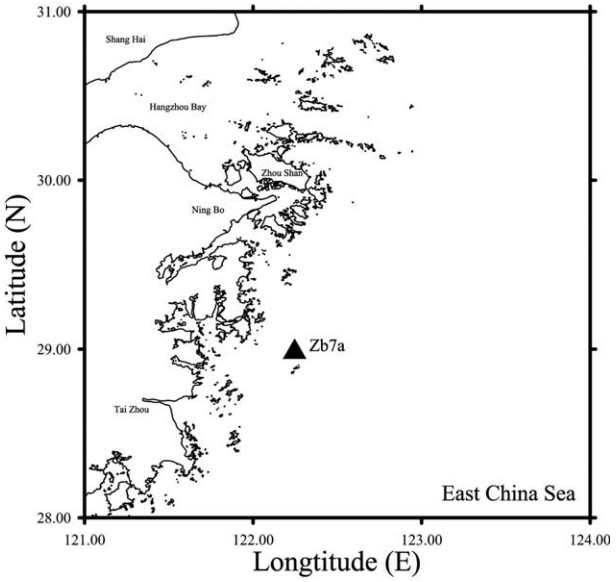

Fig. 1. Location of sampling station. Triangle: Zb7a, 28.9835° N, 122.2465° E.

Results

General features of the P. donghaiense bloom

The cell density of *P. donghaiense* increased from 1.5 × 10^5 on May 10 to 3.0 × 10^7 cells/l on May 21, 2014, while the cell density of other phytoplankton species remained relatively stable, ranging from 1.6 × 10^6 to 7.4 × 10^6 cells/l (Fig. 2). Chlorophyll *a* (Chl *a*) concentration increased from 2.12 μg/l on May 10 to 6.20 μg/l on May 21. Bacterial abundance reached the highest density (5.19 × 10^8 cells/l) on May 15, and decreased to 2.48 × 10^8 cells/l on May 21 (Fig. 2).

Concentrations of nitrate, nitrite and ammonium decreased significantly from May 15 to 21 whereas the concentration of phosphate increased greatly (Table 1). Temperature and salinity also increased with the bloom process while concentrations of silicate and dissolved oxygen decreased slightly.

Community structure of bacterioplankton in the different blooming phases

The bacterioplankton community structure was assessed using the bacterial hypervariable region V4 of the 16S rRNA gene. Operational taxonomic unit (OTU)-based composition of the bacterial community changed significantly from the middle- to the late-blooming phase (Supporting Information Fig. S1), and bacterial diversity decreased sharply in the late-blooming phase (Fig. 3 and Supporting Information Fig. S2). 16S rRNA sequencing results indicated that the predominant phyla/classes in the middle-blooming phase were *Gammaproteobacteria* (41.50% relative abundance), which was dominated by the SAR86 clade (21.60%) and the oligotrophic marine *Gammaproteobacteria* (OMG) group (3.65%), followed by the *Alphaproteobacteria* (33.58%), including the *Rhodobacteraceae* (16.09%); the SAR11 clade (9.70%); the *Fibrobacteres-Chlorobi-Bacteroidetes* (FCB) group (11.42%) and the *Actinobacteria* (8.84%).

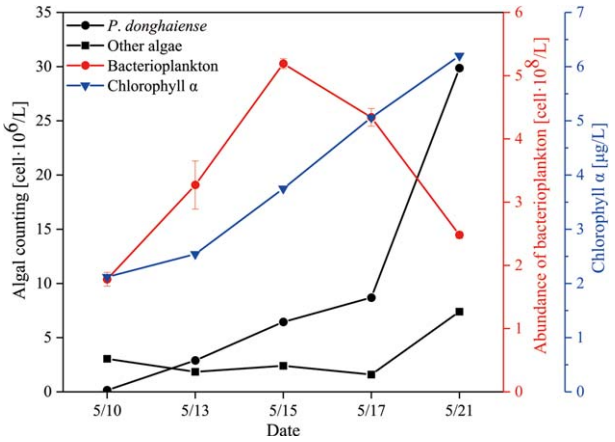

Fig. 2. Abundance of bacterioplankton (circle with red line), cell densities of *P. donghaiense* (circle with black line) and other phytoplankton species (square with black line). The concentrations of chlorophyll *a* are also labelled (triangle with blue line). [Colour figure can be viewed at wileyonlinelibrary.com]

Table 1. Environmental parameters of the samples.

Sample name	Temperature (°C)	Salinity	Oxygen saturation (mg/l)	Chl *a* (μg/l)	Silicate (μmol/l)	Phosphate (μmol/l)	Ammonium (μmol/l)	Nitrate (μmol/l)	Nitrite (μmol/l)
MS515	18.78	28.52	7.85	3.75	18.17	0.07	8.48	13.18	1.09
MS521	19.19	29.63	7.52	6.20	14.08	0.21	3.47	2.50	0.58

A small proportion of other ubiquitous bacterial groups, such as the *Alteromonadaceae*, *Pseudoalteromonadaceae*, *Oceanospirillaceae*, *Chromatiaceae*, *Pseudomonadaceae Methylophilaceae*, *Comamonadaceae*, *Bacteriovoracaceae* and *Puniceicoccaceae* were also detected. In contrast, the *Pseudoalteromonadaceae* (79.26%) dominated the bacterial community in the late-blooming phase (Fig. 3), and the *Alteromonadaceae* also occupied a certain proportion (6.79%). Other bacterial groups, such as the *Opitutaceae*, *Aurantimonadaceae*, *Lactobacillaceae* and *Micromonosporaceae*, were detected only in the late-blooming phase. The protein origins exhibited a similar bacterial population composition to the 16S rRNA sequencing results in both phases (Fig. 3).

Protein functions in the different blooming phases

A semiquantitative proteomic analysis based on normalized spectral counting was performed to compare the metabolic activities of bacterial groups between the two blooming phases. The comparison of bacterial metabolic clusters between the middle- (sample MS515) and late- (sample MS521) blooming phases is shown in Fig. 4. Proteins in all metabolic categories could be found in both samples. Membrane proteins, transporters, especially TonB-dependent receptors (TBDRs), and energy metabolism associated proteins were the major components not only in terms of their protein numbers, but also the proportions of spectral counts. The list of bacterial proteins identified for the MS515 and MS521 samples are shown in Supporting Information Tables S1 and S2.

In sample MS515, non TBDR transporters (20.53%), TBDR (16.26%), membrane protein (15.95%), energy metabolism (13.43%), stress (5.34%), translation (4.82%) and carbon metabolism (4.39%) were the major functional categories (Fig. 4). Hypothetical proteins also occupied high proportions in both spectral counts (11.89%) and protein number (15.55%). Other spectra were distributed mainly among replication/transcription (2.62%), ribosomes (1.61%), protein chaperones (1.05%), carbon fixation and central carbon metabolism (0.86%), nitrogen metabolism (0.73%), lipid metabolism (0.18%), sulfur metabolism (0.18%) and proteolysis (0.16%).

In sample MS521, TBDR was the most abundant protein group and 152 TBDR proteins accounted for 43.24% of the total spectral counts (Fig. 4). Proteins assigned to membrane protein, transporter, energy metabolism, carbon fixation and central carbon metabolism, and translation occupied 14.74%, 6.54%, 5.56%, 5.39% and 4.48% of the total spectral counts. Hypothetical proteins accounted for 6.57% of the total spectral counts. Other spectra were assigned to ribosomes (3.42%), proteolysis (2.78%), replication/transcription (1.84%), nitrogen metabolism (1.55%), carbon metabolism (1.44%), lipid metabolism (0.80%), protein chaperones (0.78%), stress (0.59%), phosphate metabolism (0.14%), cell structure (0.08%) and sulfur metabolism (0.04%).

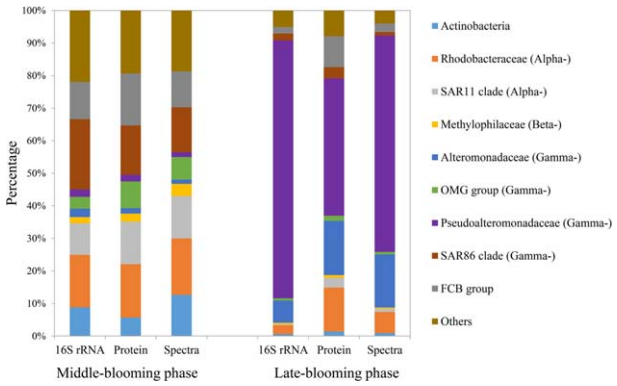

Fig. 3. The composition of major bacterioplankton groups in the middle-blooming phase (left) and late-blooming phase (right) of *P. donghaiense*.

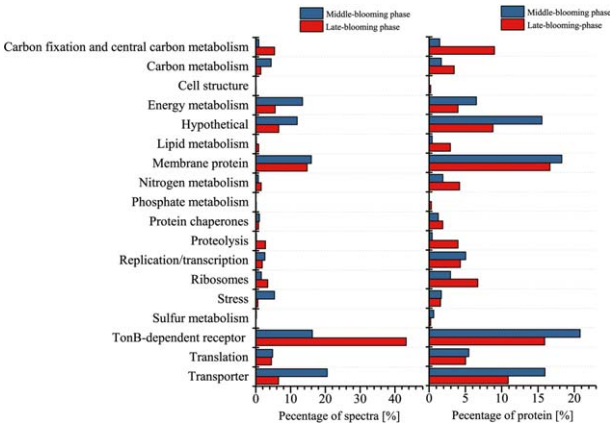

Fig. 4. Percentage of spectral counts and protein number involved in related biological processes in the middle-blooming phase (blue) and late-blooming phase (red) of *P. donghaiense*.

Transporters in the different blooming phases

A large number of transport proteins, which translocate a variety of substrates, were identified in both samples (Table 2). In sample MS515, ATP-binding cassette (ABC) transporters were abundant in the SAR11 clade, *Rhodobacteraceae* and *Actinobacteria*, but their abundance was low in the SAR116 clade. TBDRs were frequently detected in the SAR86 clade. TBDRs from the FCB group and OMG group also occupied a certain proportion. In contrast, abundances of ABC transporters from the SAR11 clade, *Rhodobacteraceae*, *Actinobacteria*, *Pseudoalteromonadaceae* and OMG group were low in sample MS521. However, TBDRs from the *Pseudoalteromonadaceae* and *Alteromonadaceae* dominated the transporters. Spectra of the sodium/solute symporter (SSS) from the SAR11 clade, and tripartite tricarboxylate transporter (TTT) and tripartite ATP-independent periplasmic (TRAP) transporter from the SAR11 clade and *Rhodobacteraceae* were also detected in both blooming phases.

Discussion

Bacterial abundance and diversity during the blooming period

The dynamics of a bacterioplankton community and close correlation between bloom-forming cells and bacteria are reported during a diatom bloom process (Needham and Fuhrman, 2016). Our study found that both bacterial abundance and composition varied dynamically during a dinoflagellate bloom: bacterial abundance increased with bloom development and peaked in the middle-blooming phase, then declined in the late-blooming phase. Meanwhile, the diversity of the bacterial community decreased significantly from the middle-blooming phase to the late-blooming phase. Pearson correlation analysis indicated that bacterial abundance was not significantly associated with environmental parameters (Supporting Information Table S4), and thus some other factors may have caused the variations of bacterial abundance and composition during the bloom. Various types of phytoplankton-originated dissolved organic matter are identified in the ocean, and bacteria are the major consumers (Amon and Benner, 1996). Bacteria can quickly utilize phytoplankton-originated organic matter which results in the explosive proliferation of bacteria during the phytoplankton bloom (Bell and Kuparinen, 1984; Tada *et al*., 2011; Teeling *et al*., 2012; Tan *et al*., 2015). Substrate-controlled succession of bacterioplankton populations and a dynamic succession of populations at genus level are observed during a diatom bloom (Teeling *et al*., 2012). Protein-like and humic-like dissolved organic matter produced by *P. donghaiense* are also reported (Zhao *et al*., 2009). Thus, it could be postulated that the variety of substrates in different blooming phases might regulate the abundance and diversity of bacteria, but this needs further study.

Interestingly, the *Pseudoalteromonadaceae* exclusively dominated the bacterioplankton community in the late-blooming phase. This group is widespread in the ocean and is tightly associated with phytoplankton blooms (Yang *et al*., 2012; Teeling *et al*., 2016). Many species of this family produce a variety of primary and secondary metabolites including hydrolytic enzymes, cyclic peptides, exopolymers, phenolic and pyrrole-containing alkaloids, and unusual brominated compounds with antibacterial and antiviral properties, which enable them to adapt to dissimilar ecological habitats in marine environments (Ivanova *et al*., 2014). Some bacterial species affiliating with this group are known to be associated with dinoflagellates and influence their growth or cyst formation (Adachi *et al*., 2002; Ferrier *et al*., 2002). In addition, many *Pseudoalteromonadaceae* species show algicidal activities to one or more specific algal species (Lovejoy *et al*., 1998; Kim *et al*., 1999; Egan *et al*., 2001), and are involved in bloom termination (Wichels *et al*., 2004). Some species from the *Pseudoalteromonadaceae* with algicidal capability are also isolated from surface seawater during a *P. donghaiense* bloom (Su *et al*., 2011). Our study showed that proteins associated with proteolysis, e.g., amidohydrolase, serine protease and peptidase, were relatively abundant (2.42% of the spectra) in the *Pseudoalteromonadaceae* in the late-blooming phase. Overall, these studies suggested a close interaction between the *Pseudoalteromonadaceae* and *P. donghaiense* during the late-blooming phase: the *P. donghaiense* bloom provided an ideal environment for bacterial growth, while certain *Pseudoalteromonadaceae* species might control the bloom process.

Metabolic activities of the bacterioplankton in the middle-blooming phase

Nutrient scavenging is important for bacterial growth during the phytoplankton bloom process (Teeling *et al*., 2012). Our results showed that different bacterial clades had unique nutrient uptake strategies to ensure their proliferation during the dinoflagellate bloom through different transporters.

In our study, taurine ABC transporters from the *Rhodobacteraceae* and SAR11 clade were detected in the middle-blooming phase. Taurine can supply bacteria with carbon, nitrogen and sulfur, but the capability to utilize these elements differs among bacteria. For example, the SAR11 clade cannot use taurine as a sulfur source (Masepohl *et al*., 2001; Tripp *et al*., 2008; Schwalbach *et al*., 2010). Taurine transporters are frequently detected in the Sargasso Sea and South China Sea (Sowell *et al*., 2009; Dong *et al*., 2014). In the coastal waters of the Antarctic Peninsula, transporters and degradation enzymes for

Table 2. Transporter proteins and spectral relative abundance for different substrates detected in the metaproteome.

Sample name	Bacterial group	ABC						TBDR	SSS	TRAP	TTT	Others
		Taurine	Sugar	Spermidine/ putrescine	Glycine betaine	(Branched-chain) amino acid	Others					
MS515	Actinobacteria	–	6 (3.55%)	–	–	2 (3.45%)	3 (1.82%)	–	–	–	–	–
	Rhodobacteraceae (Alpha-)	1 (0.12%)	1 (0.05%)	–	–	9 (1.98%)	7 (0.66%)	–	–	4 (0.30%)	1 (0.30%)	–
	SAR11 clade (Alpha-)	4 (1.21%)	–	3 (0.40%)	1 (0.07%)	6 (1.45%)	2 (0.51%)	–	11 (2.71%)	4 (0.31%)	2 (0.55%)	1 (0.05%)
	SAR116 clade (Alpha-)	–	1 (0.16%)	–	–	2 (0.24%)	–	–	–	–	–	–
	FCB group	–	–	–	–	–	–	14 (1.54%)	–	–	–	–
	Alteromonadaceae (Gamma-)	–	–	–	–	–	–	2 (0.09%)	–	–	–	–
	OMG group (Gamma-)	–	–	–	–	1 (0.07%)	–	14 (1.56%)	–	–	–	–
	Pseudoalteromonadaceae (Gamma-)	–	–	–	–	–	–	2 (0.14%)	–	–	–	–
	SAR86 clade (Gamma-)	–	–	–	–	–	–	48 (10.44%)	–	–	–	1(0.14%)
	Prochlorococcaceae	–	–	–	–	–	–	4 (0.40%)	–	–	–	2 (0.21%)
	Others	–	–	–	–	–	1 (0.09%)	15 (2.10%)	–	–	–	–
MS521	Actinobacteria	–	3 (0.20%)	–	–	2 (0.37%)	1 (0.09%)	–	–	–	–	–
	Rhodobacteraceae (Alpha-)	2 (0.06%)	2 (0.05%)	–	–	6 (0.55%)	19 (0.78%)	–	–	6 (0.14%)	2 (0.08%)	–
	SAR11 clade (Alpha-)	3 (0.13%)	–	3 (0.12%)	–	3 (0.13%)	2 (0.04%)	–	8 (0.19%)	4 (0.21%)	1 (0.02%)	1 (0.05%)
	SAR116 clade (Alpha-)	–	2 (0.20%)	–	–	1 (0.01%)	–	–	–	–	–	–
	FCB group	–	–	–	–	–	–	14 (0.36%)	–	–	–	–
	Alteromonadaceae (Gamma-)	–	–	–	–	–	–	41 (9.54%)	–	–	–	5 (0.14%)
	OMG group (Gamma-)	–	–	–	–	1 (0.01%)	–	10 (0.21%)	–	–	–	–
	Pseudoalteromonadaceae (Gamma-)	–	–	–	–	–	4 (0.24%)	54 (31.85%)	4 (0.13%)	–	–	15 (2.42%)
	SAR86 clade (Gamma-)	–	–	–	–	–	–	24 (0.90%)	–	–	–	1 (0.01%)
	Prochlorococcaceae	–	–	–	–	–	–	4 (0.07%)	–	–	–	1 (0.01%)
	Others	–	–	–	–	–	2 (0.11%)	5 (0.30%)	–	–	–	–

© 2017 Society for Applied Microbiology and John Wiley & Sons Ltd,

taurine are also detected from a range of bacterial species (Williams *et al*., 2012). These results suggested that taurine produced by the blooming cells might be an important nutrient source for heterotrophic bacteria.

Glycine betaine ABC transporter was detected only from the SAR11 clade in the middle-blooming phase. Glycine betaine serves not only as a common osmolyte in phytoplankton or macroalgae but also as carbon and energy sources in bacteria (Smith *et al*., 1988; Keller *et al*., 1999). It can be catabolized into glycine and this degradation is of great importance for the SAR11 clade (Tripp *et al*., 2009). A large number of amino acid and polyamine (putrescine/spermidine) ABC transporters that derive from the *Rhodobacteraceae* and SAR11 clade imply that bacteria can use these organic solutes as carbon and nitrogen sources for cell growth (Williams *et al*., 2012). Transporters for C4-dicarboxylate were detected from the *Rhodobacteraceae* and SAR11 clade, which was consistent with the prevalence of these proteins found in the Sargasso Sea (Sowell *et al*., 2009) and the coastal surface waters of the Antarctic Peninsula (Williams *et al*., 2012), implying that C4-dicarboxylate is an important and cosmopolite carbon source for these bacterial groups. *Actinobacteria* massively decompose plant carbohydrates during a bloom (Penn *et al*., 2014). A large proportion of sugar ABC transporters with a predicted substrate of alpha-glucoside were detected in *Actinobacteria* in the middle-blooming phase, indicating that they were more likely to utilize glucoside as the carbon source. Unlike ABC transporters, which transport substrates through ATP hydrolysis, an electrochemical ion gradient is utilized by TRAP and TTT transporters to drive solute uptake (Winnen *et al*., 2003; Moran *et al*., 2007; Mulligan *et al*., 2009). A few transporters detected in our study demonstrated that carboxylic acids were not the prior substances for bacterial uptake during the bloom. Moreover, SSS was identified mainly from the SAR11 clade, and SSS can catalyse the uptake of various solutes including sugars, proline, pantothenate and iodide into cells (Jung, 2002). These results indicated that the SAR11 clade can utilize various substrates via different ways. Similar SAR11 transporters are also found in the proteomes from other marine regions (Morris *et al*., 2002; Sowell *et al*., 2009), suggesting that diverse nutrient uptake strategies are beneficial to the survival of the SAR11 clade in the fierce nutrient competitive environment.

TBDRs can transport dissolved organic matter, iron/heme-binding protein or siderophores/vitamins into Gram-negative bacteria (Tang *et al*., 2012). Abundant TBDRs were assigned to the SAR86 clade, and the OMG and FCB groups in the middle-blooming phase. Following the classification reported by Tang and colleagues (2012), transporters of group I for DOM (7% of the total spectra) and group II for siderophores/vitamins (2%) comprised all TBDRs detected in the SAR86 clade (Supporting Information Fig. S3). Homologues of TBDRs in the SAR86 genomes with predicted substrates of sulfolipids and polyhydroxyalkanoates (Dupont *et al*., 2012) were detected, indicating the utilization of these distinct carbon compounds by the SAR86 clade. Other organic substrates including xylose, xylan, phytate, sulfur esters and arabinose were also predicted (Supporting Information Table S5), suggesting that these compounds might support the abundance of the SAR86 population (Fig. 3). Moreover, the detection of SAR86 TBDRs for vitamin B12 in our study was consistent with the absence of a vitamin synthesis pathway that is one of the evidences for metabolic streamlining in the SAR86 clade (Dupont *et al*., 2012). A comparable abundance of TBDRs in the OMG (1.56%) and FCB groups (1.54%) in our study were also supported by *in situ* metaproteome studies in the North Sea (Teeling *et al*., 2012) and South China Sea (Dong *et al*., 2014). TBDRs from the FCB groups were predicted to be affiliated with biopolymers such as starch, chondroitin sulfate, hyaluronic acid, oligosaccharides, digested proteins and fibronectin, while the OMG groups might favour arabinose, sulfate esters, vitamins B1 and B12 and catecholates (Supporting Information Table S5). These results indicated the different nutrient niches between the FCB and OMG groups in the middle-blooming phase.

Methanol dehydrogenase from the OM43 clade matched 2.38% of all spectra in the middle-blooming phase, indicating that this clade actively utilized methanol as a carbon and energy source. Methanol is thought to be produced by the phytoplankton and is regarded as a major source of carbon and energy for the OM43 clade in coastal ecosystems (Giovannoni *et al*., 2008; Sowell *et al*., 2011), which enables the OM43 clade to avoid the nutrient competition from other bacterial species. The proportion of the OM43 clade in the middle-blooming phase supported the conclusion that the abundance of this clade in the coastal ecosystem is increased during phytoplankton blooms (Morris *et al*., 2006). Although a low proportion of the OM43 clade was detected in the late-blooming phase, most of the OM43 clade spectra assigned to methanol dehydrogenase showed that they had a steady and exclusive nutrient utilization strategy.

Proteins, such as translocating pyrophosphatase and ATP synthase involved in energy metabolism presented higher abundances in the middle-blooming phase, implying an active energy production of bacteria, which provided sufficient energy for substrate remineralization, production storage, cell motility, waste removal, cellular machinery repair and subsequent bacterial growth (Del Giorgio and Cole, 1998; Carlson *et al*., 2007). The active energy metabolism of the *Rhodobacterales* and SAR11 clade in this phase directly corresponded to the high proportions of the

bacterioplankton community, while a large proportion of detected spectra related to energy metabolism were assigned to the predominant *Pseudoalteromonadaceae* in the late-blooming phase. A study on microbial community gene expression within colonies of *Trichodesmium* suggests that energy conservation is critical to procaryotic organisms during blooms along with the high transcriptional expression of energy metabolism from *Trichodesmium* (Hewson *et al.*, 2009). Our results implied that the bacterial capability of energy metabolism correlated with the dynamics of the bacterioplankton community during the *P. donghaiense* blooming process. Blooming cells of *P. donghaiense* might provide abundant substrates for bacterial energy metabolism, which subsequently enhanced bacterial cell growth.

Approximately 3.3% of spectra were assigned to selenium-binding protein from a gammaproteobacterium HTCC2080 in the middle-blooming phase. The function of this protein is not yet specified (Zhang *et al.*, 2008). Genomic context of this gene in HTCC2080 shows that its neighbourhood genes are cytochrome-c peroxidase associated with the reduction of hydrogen peroxide, suggesting that selenium-binding protein might play a role in response to oxidative stress caused by hydrogen peroxide in HTCC2080.

Metabolic activities of the bacterioplankton in the late-blooming phase

Our results indicated that the *Pseudoalteromonadaceae* dominated the bacterioplankton community in the late-blooming phase. Some *Pseudoalteromonadaceae* species show specific algicidal activity to *P. donghaiense* by algal-lytic compounds with beta-glucosidase activity (Kim *et al.*, 2009; Seong and Jeong, 2013). In our study, beta-glucosidase, an extracellular enzyme catalyzing the hydrolysis of glycosidic bonds, was detected from the *Pseudoalteromonadaceae* only in the late-blooming phase, suggesting an active role of this group in lysing *P. donghaiense* cells. Beta-glucosidase might be involved in the degradation of the *P. donghaiense* cell walls, which are composed mainly of cellulose, laminarins, alginic acid and fucoidans (Warren, 1996), and subsequently resulted in the termination of the *P. donghaiense* bloom (Fig. 5).

Spectra of serine protease from the *Pseudoalteromonadaceae* were also frequently detected in the late-blooming phase, and extracellular serine protease produced by *Pseudoalteromonas* sp. strain A28 can cause diatom cell lysis (Lee *et al.*, 2000). Bacterial excreted serine protease also induces cell motility reduction of the dinoflagellate *Lingulodinium polyedrum* (Mayali *et al.*, 2008). The frequent detection of serine protease in the

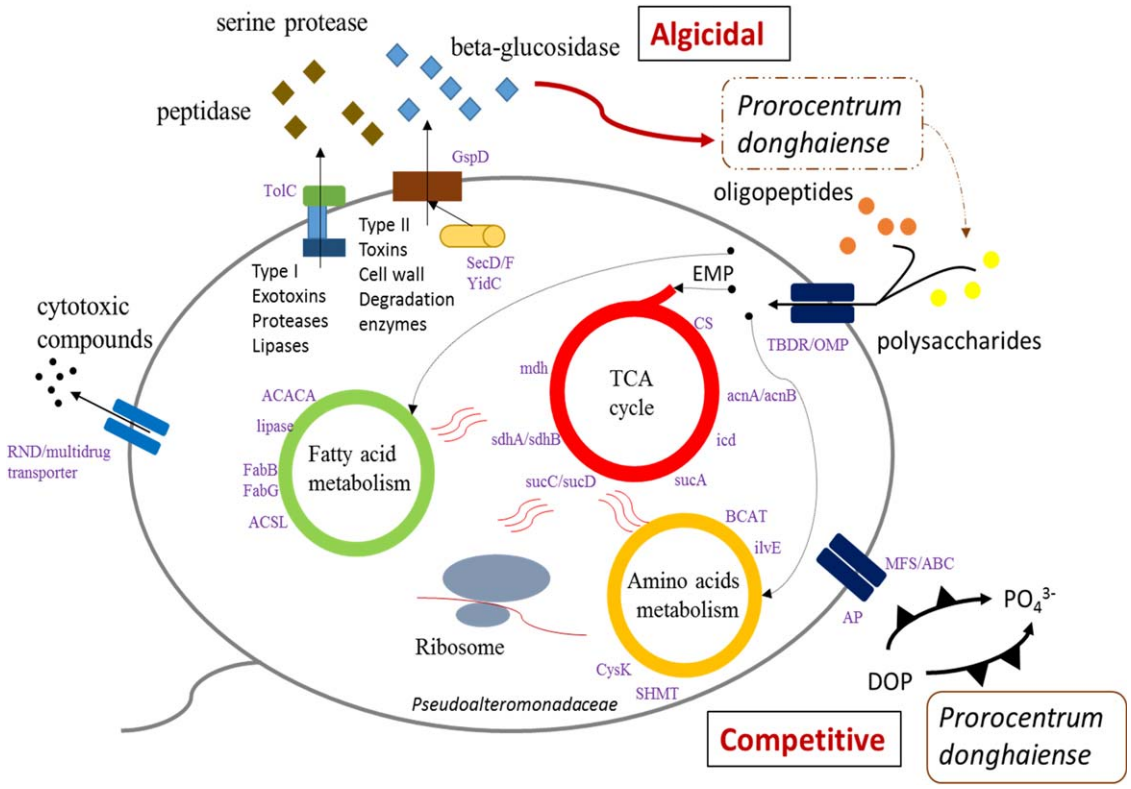

Fig. 5. Schematic summary of the major metabolic activities occurring in the *Pseudoalteromonadaceae* in the late-blooming phase of *P. donghaiense*.

Pseudoalteromonadaceae in the late-blooming phase indicated that this bacterial group might have an adverse effect on *P. donghaiense* and other phytoplankton species (Fig. 5).

Two proteins, TolC and GspD from type I and II secretion systems were detected from the *Pseudoalteromonadaceae*. Type I and II secretion systems mainly secrete or specifically deliver toxins, proteases, cellulases and lipases to the extracellular environment (Buchanan, 2001; Johnson *et al*., 2006). Bacteria from the *Pseudoalteromonadaceae* might secrete *in vivo* substances through these systems to affect other microorganisms, for example, inhibiting other bacterial growth or degrading algal cells (Delepelaire, 2004; Evans *et al*., 2008). In addition, the resistance nodulation division family transporter and the multidrug transporter, the important exporters of biological metabolites and antimicrobial compounds which can protect bacterial cells from antibiotics to improve bacterial viability (Tikhonova *et al*., 2002), were identified only from the *Pseudoalteromonadaceae* in the late-blooming phase. These results suggested that the *Pseudoalteromonadaceae* have strong environmental adaptabilities compared to other bacterial groups which enable them to outcompete their rivals.

In our study, hydrolases, such as glycosyl hydrolase family 16 and amidohydrolase from the *Pseudoalteromonadaceae*, and subtilase and amidohydrolase from *Alteromonadaceae*, were identified in the late-blooming phase. These enzymes are involved in the cleavage of polysaccharides, amide bonds or peptide bonds. A substantial amount of spectra assigned to these enzymes in the late-blooming phase reflected active hydrolysis of small molecular compounds, such as glucans, galactans, amides or peptides, which provided nutrients for the growth of bacteria from the *Pseudoalteromonadaceae* and *Alteromonadaceae*. Consistently, TBDRs for sugars, e.g., arabinose, xylose, xylan, chito-oligosaccharide, maltose and maltodextrin, were frequently detected from the *Pseudoalteromonadaceae* and *Alteromonadaceae*, which provided diverse carbon sources for the growth of both bacterial groups. TBDRs for vitamins (such as thiamin and B12), as well as siderophores, were also detected, suggesting that the cell demands for vitamins and iron could be fulfilled via these TBDRs. Moreover, nearly all the TCA cycle enzymes were detected in the *Pseudoalteromonadaceae*, and proteins associated with ribosomes and lipid metabolism were also abundant, indicating active energy metabolism and biosynthesis of proteins and lipids. Overall, these results indicated that the *Pseudoalteromonadaceae* dominated substrate utilization in the bacterioplankton community and presented an exuberant vitality in the late-blooming phase.

Two phosphorus utilizing proteins, phosphate ABC transporter and alkaline phosphatase were detected from the *Pseudoalteromonadaceae*, indicating that this bacterial group could utilize both organic and inorganic phosphorus under ambient phosphorus deficient conditions (Fig. 5). As an essential nutrient for life, the deficiency of phosphorus can limit both primary and bacterial secondary production (Vadstein, 2000). The intense competition for nutrients between the bacteria and phytoplankton causes a negative effect on phytoplankton growth (Joint *et al*., 2002; Aharonovich and Sher, 2016). In our study, the phosphate concentration in the late-blooming phase increased greatly compared to the middle-blooming phase, but it still limited phytoplankton growth (Liu *et al*., 2013). Transcripts of phosphate ABC transporter and alkaline phosphatase were also detected in the *in situ P. donghaiense* blooming cells (our unpublished data). These results suggested that the predominant *Pseudoalteromonadaceae* in the late-blooming phase might cause stress on the phosphorus uptake of *P. donghaiense* cells.

Overall, our study indicated that the bacteria from the *Pseudoalteromonadaceae* possess inherent advantages, such as algae-lytic ability, an efficient nutrient transport system and antibacterial and self-protection mechanisms (Fig. 5), which enable them to outcompete other bacterial groups and dominate the bacterial community in the late-blooming phase. Meanwhile the *Pseudoalteromonadaceae* might play an important role in regulating the termination of a dinoflagellate bloom. The future work will be focussed on the isolation of key bacterial species from the *Pseudoalteromonadaceae* and the study of their genetics and ecological functions.

Conclusions

Our results showed that the composition and metabolic activity of the bacterioplankton varied dynamically with the development of a *P. donghaiense* bloom. A diverse substrate utilization strategy might be responsible for the succession of bacterioplankton populations during the blooming period. Interestingly, the *Pseudoalteromonadaceae* dominated the bacterial community in the late-blooming phase and presented active metabolism. This bacterial group is known to be closely associated with phytoplankton blooms and their algicidal activity might be responsible for the collapse of *P. donghaiense* blooms. Thus, a comprehensive study of this bacterial group is necessary so as to help to unveil their roles in the termination of phytoplankton blooms. It should be noted that we could not investigate the metaproteomes of algae-attached bacteria owing to the low extraction yield of the attached bacterial proteins. Future research should use integrated approaches, such as metaproteomics, metagenomics and metabolomics to improve our understanding of both free living and attached bacteria during phytoplankton blooms, combining a range of techniques, to explore and link the microbial diversity and activity so as to ultimately understand the relationship between bacteria and bloom-forming phytoplankton species.

Experimental procedures

Sample collection

A dinoflagellate bloom caused by *P. donghaiense* occurred in the coastal East China Sea from May 10 to June 3, 2014 (Huang *et al*., 2014), and our survey was conducted from May 10 to 21. Two samples (MS515 and MS521) were collected at station Zb7a (Fig. 1 and Supporting Information Table S3) on May 15, 2014 (the middle-blooming phase) and May 21, 2014 (the late-blooming phase). The blooming phase was determined based on the cell density of *P. donghaiense* in the seawater. 125 l surface seawater (2 m) was first filtered through 200 μm pore size mesh (SEFAR NITEX03–200; Sefar, Switzerland) to remove zooplankton, and then filtered through 1.6 μm pore size GF/A glass fibre filters (142-mm diameter, Whatman™, GE Healthcare, UK) to remove phytoplankton. Finally, bacteria were collected onto 0.2 μm GTTP polycarbonate membranes (Isopore™, Millipore Corp., USA). 5 l of seawater were enriched for 16S rRNA gene sequencing, and 120 l for metaproteomic analysis.

Measurements of environmental parameters

Salinity, temperature and dissolved oxygen during the blooming period were measured using a SeaBird 911 plus CTD instrument. Chl *a* concentration was determined using a Turner Trilogy® fluorometer. Nutrients, including silicate, phosphate, ammonium, nitrate and nitrite were analysed using a continuous flow analyser (SAN^{++}, Skalar, The Netherlands), and cell densities of *P. donghaiense* and other phytoplankton species were counted under an optical microscope.

Bacterial abundance

To count the bacterioplankton, three 2 ml seawater samples, which were prefiltered through a 1.6 μm pore size GF/A glass fibre with 2% glutaraldehyde, were stored in liquid nitrogen. Bacterial cells were stained with SYBR Green I in anhydrous dimethylsulfoxide and incubated in the dark for 15 min. Bacterial abundance in each sample was determined using a BD FACSAria Flow Cytometer (Becton Dickinson, USA) following the protocol described previously (Marie *et al*., 1999).

DNA extraction, PCR amplification and sequencing

Bacterial DNA was extracted following the protocol described elsewhere (Liu *et al*., 2007). Universal V4 region primers for 16S rRNA genes were used (Dethlefsen *et al*., 2008; Huse *et al*., 2008). PCR reactions were performed in a 30 μl reaction system containing 15 μl Phusion® High-Fidelity PCR Master Mix (NEB, Beverly, USA), 0.2 μmol of each primer and 10 ng DNA template. The amplification process included 60 s of predegeneration at 98°C; 30 cycles of 98°C for 10 s, 50°C for 30 s, 72°C for 60 s; and finally, extension at 72°C for 300 s. The PCR products were purified using a GeneJET Gel Extraction Kit (Thermo Fisher Scientific, USA), and an NEB Next® Ultra™ DNA Library Prep Kit was used for the library construction. The library quality was assessed using a Qubit@ 2.0 Fluorometer (Invitrogen, Q32866) and the Agilent Bioanalyzer 2100 system (Agilent Technologies, USA). The eligible library was sequenced using the Illumina MiSeq platform (Illumina, USA).

Protein extraction and quantification

Protein extraction and quantification followed the method reported previously (Dong *et al*., 2009). Briefly, the membrane with bacteria was transferred into a 2 ml centrifuge tube with protein lysis buffer, and then shaken for 15 min in an ultrasonic oscillator with ice-cold water. Then, the mixture was sonicated in a bath sonicator for two 4-min cycles, and then centrifuged with 15 000 g for 30 min at 4°C. The supernatant was precipitated with ice-cold 20% trichloroacetic acid in acetone for at least 12 h. The resultant pellet was rinsed twice with ice-cold acetone and air-dried after centrifugation. Finally, the powder was dissolved in rehydration buffer. The protein concentration was quantified using the Bradford method (Kruger, 2009).

Metaproteomic analysis

50-μg protein was reduced by trypsin in a 20:1 (w/w) protein/enzyme ratio for 12 h at 37°C. The digested peptide fractionation was performed using SCX chromatography with an LC-20AB HPLC Pump system (Shimadzu, Japan). The elutropic peptides underwent nanoelectrospray ionization using tandem mass spectrometry (MS/MS) in Q-EXACTIVE (Thermo Fisher Scientific, USA) coupled online to the HPLC system. Peptides were selected using MS/MS high-energy collision dissociation operating mode, and ion fragments were detected in the Orbitrapat 17 500 resolution. The top 15 abundant precursor ions in the MS survey scan were adopted for the MS2 analysis. The electrospray voltage was 1.6 kV. The automatic gain control targets for MS and MS2 were $3e^6$ and $1e^5$, and the MS and MS2 *m/z* scan ranges were 350–2000 and 100–1800 Da.

Bioinformatics analysis

Paired-end reads from the original DNA fragments were merged using FLASH (Magoč and Salzberg, 2011). The raw tags with a continuous high-quality base length less than 75% of the total tag length and chimeric sequences were removed (Caporaso *et al*., 2010). Effective tag analysis was performed using the UPARSE software package (Edgar, 2013). Sequences with $\geq$ 97% similarity were assigned to the same OTUs. An RDP classifier was used to annotate taxonomic information for each OTU representative sequence by matching with the GreenGene database (http://greengenes.lbl.gov/cgi-bin/nph-index.cgi). The threshold value ranged from 0.8 to 1.0.

MS/MS data analysis and protein identification were performed using the Mascot search engine (version 2.3.02) against a Tara database containing 40 090 133 protein sequences (translated from OM-RGC, http://ocean-microbiome.embl.de/companion.html). The tolerance of intact peptide masses was 0.1 Da and that of fragmented ions 0.05 Da. One missed cleavage in the trypsin digests was allowed. Peptides with significance scores ($\geq$ 20) at the 99%

confidence interval in a Mascot probability analysis were counted as identified.

Matched peptide sequences were annotated with Blast2GO (Conesa *et al*., 2005). Proteins with at least two peptides and one unique peptide were considered for further analysis (Sowell *et al*., 2009; Zhang *et al*., 2015). Categorical annotation referred to the non-redundant (NR) database protein description, the participation of the Kyoto Encyclopedia of Genes and Genomes (KEGG) pathway and the biological process of COG (the database of Clusters of Orthologous Groups of proteins) with molecular function and cellular components (Zhang *et al*., 2016). Substrates of TBDRs were predicted based on the top BLASTp hit against standard or characterized TBDRs with known substrates following a previous study (Tang *et al*., 2012). Comparison of detected proteins with their relative amounts between the middle- and late-blooming phases was determined with label-free quantification. Before the comparison, each protein abundance was normalized by calculating its spectra proportion in all protein spectra counts within one sample (Morris *et al*., 2010).

Acknowledgements

We gratefully acknowledge the captain and crew of the R/V *Yanping* II. This work was supported by the National Natural Science Foundation of China (Project No. 41230961 and 41425021). We thank Professor John Hodgkiss of the City University of Hong Kong for assistance with the English.

Conflict of Interest

The authors declare no conflict of interest.

References

Adachi, M., Matsubara, T., Okamoto, R., Nishijima, T., Itakura, S., and Yamaguchi, M. (2002) Inhibition of cyst formation in the toxic dinoflagellate *Alexandrium* (Dinophyceae) by bacteria from Hiroshima Bay, Japan. *Aquat Microb Ecol* **26:** 223–233.

Aharonovich, D., and Sher, D. (2016) Transcriptional response of *Prochlorococcus* to co-culture with a marine *Alteromonas*: differences between strains and the involvement of putative infochemicals. *ISME J* **10:** 2892–2906.

Amin, S.A., Parker, M.S., and Armbrust, E.V. (2012) Interactions between diatoms and bacteria. *Microbiol Mol Biol Rev* **76:** 667–684.

Amon, R.M.W., and Benner, R. (1996) Bacterial utilization of different size classes of dissolved organic matter. *Limnol Oceanogr* **41:** 41–51.

Anderson, D.M., Cembella, A.D., and Hallegraeff, G.M. (2012) Progress in understanding harmful algal blooms: paradigm shifts and new technologies for research, monitoring, and management. *Annu Rev Mar Sci* **4:** 143–176.

Bell, R.T., and Kuparinen, J. (1984) Assessing phytoplankton and bacterioplankton production during early spring in Lake Erken, Sweden. *Appl Environ Microbiol* **48:** 1221–1230.

Buchan, A., Lecleir, G.R., Gulvik, C.A., and González, J.M. (2014) Master recyclers: features and functions of bacteria associated with phytoplankton blooms. *Nat Rev Microbiol* **12:** 686–698.

Buchanan, S.K. (2001) Type I secretion and multidrug efflux: transport through the TolC channel-tunnel. *Trends Biochem Sci* **26:** 3–6.

Caporaso, J.G., Kuczynski, J., Stombaugh, J., Bittinger, K., Bushman, F.D., and Costello, E.K. (2010) QIIME allows analysis of high-throughput community sequencing data. *Nat Methods* **7:** 335–336.

Carlson, C.A., Giorgio, P.A., and Herndl, G.J. (2007) Microbes and the dissipation of energy and respiration: from cells to ecosystems. *Oceanography* **20:** 89.

Conesa, A., Gotz, S., Garcia-Gomez, J.M., Terol, J., Talon, M., and Robles, M. (2005) Blast2GO: a universal tool for annotation, visualization and analysis in functional genomics research. *Bioinformatics* **21:** 3674–3676.

Del Giorgio, P.A., and Cole, J.J. (1998) Bacterial growth efficiency in natural aquatic systems. *Annu Rev Ecol Syst* **29:** 503–541.

Delepelaire, P. (2004) Type I secretion in gram-negative bacteria. *Biochim Biophys Acta* **1694:** 149–161.

Dethlefsen, L., Huse, S., Sogin, M.L., Relman, D.A., and Eisen, J.A. (2008) The pervasive effects of an antibiotic on the human gut microbiota, as revealed by deep 16S rRNA sequencing. *PLoS Biol* **6:** e280.

Dong, H.P., Wang, D.Z., Dai, M., Chan, L.L., and Hong, H.S. (2009) Shotgun proteomics: tools for analysis of marine particulate proteins. *Limnol Oceanogr Methods* **7:** 865–874.

Dong, H.P., Hong, Y.G., Lu, S., and Xie, L.Y. (2014) Metaproteomics reveals the major microbial players and their biogeochemical functions in a productive coastal system in the northern South China Sea. *Environ Microbiol Rep* **6:** 683–695.

Dupont, C.L., Rusch, D.B., Yooseph, S., Lombardo, M.-J., Alexander Richter, R., Valas, R., *et al*. (2012) Genomic insights to SAR86, an abundant and uncultivated marine bacterial lineage. *ISME J* **6:** 1186–1199.

Edgar, R.C. (2013) UPARSE: highly accurate OTU sequences from microbial amplicon reads. *Nat Methods* **10:** 996–998.

Egan, S., James, S., Holmström, C., and Kjelleberg, S. (2001) Inhibition of algal spore germination by the marine bacterium *Pseudoalteromonas tunicata*. *FEMS Microbiol Ecol* **35:** 67–73.

Evans, F.F., Egan, S., and Kjelleberg, S. (2008) Ecology of type II secretion in marine *gammaproteobacteria*. *Environ Microbiol* **10:** 1101–1107.

Ferrier, M., Martin, J.L., and Rooney-Varga, J.N. (2002) Stimulation of *Alexandrium fundyense* growth by bacterial assemblages from the Bay of Fundy. *J Appl Microbiol* **92:** 706–716.

Giovannoni, S.J., Hayakawa, D.H., Tripp, H.J., Stingl, U., Givan, S.A., Cho, J.-C., *et al*. (2008) The small genome of an abundant coastal ocean methylotroph. *Environ Microbiol* **10:** 1771–1782.

Hewson, I., Poretsky, R.S., Dyhrman, S.T., Zielinski, B., White, A.E., and Tripp, H.J. (2009) Microbial community gene expression within colonies of the diazotroph, *Trichodesmium*, from the Southwest Pacific Ocean. *ISME J* **3:** 1286–1300.

Huang, B., Shao, J.B., Wei, N., and Wang, Y.M. (2014) Ecological studies during occurrence of dinoflagellate blooms in East China Sea spring 2014. *Ecol Environ* **23:** 1457–1462.

Huse, S.M., Dethlefsen, L., Huber, J.A., Welch, D.M., Relman, D.A., Sogin, M.L., and Eisen, J.A. (2008) Exploring

microbial diversity and taxonomy using SSU rRNA hypervariable tag sequencing. *PLoS Genet* **4:** e1000255.
Ivanova, E.P., Ng, H.J., and Webb, H.K. (2014) The family *Pseudoalteromonadaceae*. In *The Prokaryotes*. Berlin, Heidelberg: Springer, pp. 575–582.
Johnson, T.L., Abendroth, J., Hol, W.G., and Sandkvist, M. (2006) Type II secretion: from structure to function. *FEMS Microbiol Lett* **255:** 175–186.
Joint, I., Henriksen, P., Fonnes, G.A., Bourne, D., Thingstad, T.F., and Riemann, B. (2002) Competition for inorganic nutrients between phytoplankton and bacterioplankton in nutrient manipulated mesocosms. *Aquat Microb Ecol* **29:** 145–159.
Jung, H. (2002) The sodium/substrate symporter family: structural and functional features. *FEBS Lett* **529:** 73–77.
Keller, M.D., Kiene, R.P., Matrai, P.A., and Bellows, W.K. (1999) Production of glycine betaine and dimethylsulfoniopropionate in marine phytoplankton. I. Batch cultures. *Mar Biol* **135:** 237–248.
Kim, J.D., Kim, J.Y., Park, J.K., and Lee, C.G. (2009) Selective control of the *Prorocentrum minimum* harmful algal blooms by a novel algal-lytic bacterium *Pseudoalteromonas haloplanktis* AFMB-008041. *Mar Biotechnol* **11:** 463–472.
Kim, J.H., Park, J.H., Song, Y.H., and Chang, D.S. (1999) Isolation and characterization of the marine bacterium, *Alteromonas* sp. SR-14 inhibiting the growth of diatom, *Chaetoceros* species. *J Korean Fish Soc* **32:** 155–159.
Kirchman, D.L., Suzuki, Y., Garside, C., and Ducklow, H.W. (1991) High turnover rates of dissolved organic carbon during a spring phytoplankton bloom. *Nature* **352:** 612–614.
Kodama, M., Doucette, G.J., and Green, D.H. (2006) Relationships between bacteria and harmful algae. In *Ecology of Harmful Algae*. Granéli, E., Turner, J.T. (eds). Berlin, Heidelberg: Springer, pp. 243–255.
Kruger, N.J. (2009) The Bradford method for protein quantitation. In *The Protein Protocols Handbook. Totowa, NJ: Humana Press*, pp. 17–24.
Larsen, A., Flaten, G.A.F., Sandaa, R.-A., Castberg, T., Thyrhaug, R., Erga, S.R., *et al.* (2004) Spring phytoplankton bloom dynamics in Norwegian coastal waters: microbial community succession and diversity. *Limnol Oceanogr* **49:** 180–190.
Lee, S., Kato, J., Takiguchi, N., Kuroda, A., Ikeda, T., Mitsutani, A., and Ohtake, H. (2000) Involvement of an extracellular protease in algicidal activity of the marine bacterium *Pseudoalteromonas* sp. strain A28. *Appl Environ Microbiol* **66:** 4334–4339.
Liu, H.C., Shih, C.Y., Gong, G.C., Ho, T.Y., Shiah, F.K., Hsieh, C.H., and Chang, J. (2013) Discrimination between the influences of river discharge and coastal upwelling on summer microphytoplankton phosphorus stress in the East China Sea. *Cont Shelf Res* **60:** 104–112.
Liu, J.Q., Lewitus, A.J., Brown, P., and Wilde, S.B. (2008) Growth-promoting effects of a bacterium on raphidophytes and other phytoplankton. *Harmful Algae* **7:** 1–10.
Liu, Y.Q., Yao, T.D., Kang, S.C., Jiao, N.Z., Zeng, Y.H., Huang, S.J., and Luo, T.W. (2007) Microbial community structure in major habitats above 6000 m on Mount Everest. *Chinese Sci Bull* **52:** 2350–2357.
Lovejoy, C., Bowman, J.P., and Hallegraeff, G.M. (1998) Algicidal effects of a novel marine *Pseudoalteromonas* isolate (Class *Proteobacteria*, Gamma Subdivision) on harmful algal bloom species of the genera *Chattonella*, *Gymnodinium*, and *Heterosigma*. *Appl Environ Microb* **64:** 2806–2813.
Magoč, T., and Salzberg, S.L. (2011) FLASH: fast length adjustment of short reads to improve genome assemblies. *Bioinformatics* **27:** 2957–2963.
Marie, D., Partensky, F., Vaulot, D., and Brussaard, C. (1999) Enumeration of phytoplankton, bacteria, and viruses in marine samples. *Curr Protoc Cytom* **11:** 1–15.
Masepohl, B., Führer, F., and Klipp, W. (2001) Genetic analysis of a *Rhodobacter capsulatus* gene region involved in utilization of taurine as a sulfur source. *FEMS Microbiol Lett* **205:** 105–111.
Mayali, X., and Azam, F. (2004) Algicidal bacteria in the sea and their impact on algal blooms. *J Eukaryot Microbiol* **51:** 139–144.
Mayali, X., Franks, P.J.S., Tanaka, Y., and Azam, F. (2008) Bacteria-induced motility reduction in *Lingulodinium Polyedrum* (Dinophyceae) 1. *J Phycol* **44:** 923–928.
Moran, M.A., Belas, R., Schell, M.A., González, J.M., Sun, F., Sun, S., *et al.* (2007) Ecological genomics of marine *Roseobacters*. *Appl Environ Microb* **73:** 4559–4569.
Morris, R.M., Rappé, M.S., Connon, S.A., Vergin, K.L., Siebold, W.A., Carlson, C.A., and Giovannoni, S.J. (2002) SAR11 clade dominates ocean surface bacterioplankton communities. *Nature* **420:** 806–810.
Morris, R.M., Longnecker, K., and Giovannoni, S.J. (2006) *Pirellula* and OM43 are among the dominant lineages identified in an Oregon coast diatom bloom. *Environ Microbiol* **8:** 1361–1370.
Morris, R.M., Nunn, B.L., Frazar, C., Goodlett, D.R., Ting, Y.S., and Rocap, G. (2010) Comparative metaproteomics reveals ocean-scale shifts in microbial nutrient utilization and energy transduction. *ISME J* **4:** 673–685.
Mulligan, C., Geertsma, E.R., Severi, E., Kelly, D.J., Poolman, B., and Thomas, G.H. (2009) The substrate-binding protein imposes directionality on an electrochemical sodium gradient-driven TRAP transporter. *Proc Natl Acad Sci USA* **106:** 1778–1783.
Needham, D.M., and Fuhrman, J.A. (2016) Pronounced daily succession of phytoplankton, archaea and bacteria following a spring bloom. *Nat Microbiol* **1:** 16005.
Niu, Y., Shen, H., Chen, J., Xie, P., Yang, X., Tao, M., Ma, Z., and Qi, M. (2011) Phytoplankton community succession shaping bacterioplankton community composition in Lake Taihu, China. *Water Res* **45:** 4169–4182.
Penn, K., Wang, J., Fernando, S.C., and Thompson, J.R. (2014) Secondary metabolite gene expression and interplay of bacterial functions in a tropical freshwater cyanobacterial bloom. *ISME J* **8:** 1866–1878.
Schwalbach, M.S., Tripp, H.J., Steindler, L., Smith, D.P., and Giovannoni, S.J. (2010) The presence of the glycolysis operon in SAR11 genomes is positively correlated with ocean productivity. *Environ Microbiol* **12:** 490–500.
Seong, K.A., and Jeong, H.J. (2013) Interactions between marine bacteria and red tide organisms in Korean waters. *Algae* **28:** 297–305.

Smayda, T.J. (2002) Adaptive ecology, growth strategies and the global bloom expansion of dinoflagellates. *J Oceanogr* **58:** 281–294.

Smith, L.T., Pocard, J.A., Bernard, T., and Le Rudulier, D. (1988) Osmotic control of glycine betaine biosynthesis and degradation in *Rhizobium meliloti*. *J Bacteriol* **170:** 3142–3149.

Sowell, S.M., Wilhelm, L.J., Norbeck, A.D., Lipton, M.S., Nicora, C.D., Barofsky, D.F., *et al*. (2009) Transport functions dominate the SAR11 metaproteome at low-nutrient extremes in the Sargasso Sea. *ISME J* **3:** 93–105.

Sowell, S.M., Abraham, P.E., Shah, M., Verberkmoes, N.C., Smith, D.P., Barofsky, D.F., and Giovannoni, S.J. (2011) Environmental proteomics of microbial plankton in a highly productive coastal upwelling system. *ISME J* **5:** 856–865.

Su, J.Q., Yang, X.R., Zhou, Y.Y., and Zheng, T.L. (2011) Marine bacteria antagonistic to the harmful algal bloom species *Alexandrium tamarense* (Dinophyceae). *Biol Control* **56:** 132–138.

Tada, Y., Taniguchi, A., Nagao, I., Miki, T., Uematsu, M., Tsuda, A., and Hamasaki, K. (2011) Differing growth responses of major phylogenetic groups of marine bacteria to natural phytoplankton blooms in the western North Pacific Ocean. *Appl Environ Microbiol* **77:** 4055–4065.

Tan, S., Zhou, J., Zhu, X., Yu, S., Zhan, W., Wang, B., Cai, Z., and Lindell, D. (2015) An association network analysis among microeukaryotes and bacterioplankton reveals algal bloom dynamics. *J Phycol* **51:** 120–132.

Tang, K., Jiao, N., Liu, K., Zhang, Y., Li, S., and Kirchman, D.L. (2012) Distribution and functions of TonB-dependent transporters in marine bacteria and environments: implications for dissolved organic matter utilization. *PLoS One* **7:** e41204.

Teeling, H., Fuchs, B.M., Becher, D., Klockow, C., Gardebrecht, A., Bennke, C.M., *et al*. (2012) Substrate-controlled succession of marine bacterioplankton populations induced by a phytoplankton bloom. *Science* **336:** 608–611.

Teeling, H., Fuchs, B.M., Bennke, C.M., Krüger, K., Chafee, M., Kappelmann, L., *et al*. (2016) Recurring patterns in bacterioplankton dynamics during coastal spring algae blooms. *eLife* **5:** e11888.

Tikhonova, E.B., Wang, Q., and Zgurskaya, H.I. (2002) Chimeric analysis of the multicomponent multidrug efflux transporters from gram-negative bacteria. *J Bacteriol* **184:** 6499–6507.

Tripp, H.J., Kitner, J.B., Schwalbach, M.S., Dacey, J.W.H., Wilhelm, L.J., and Giovannoni, S.J. (2008) SAR11 marine bacteria require exogenous reduced sulphur for growth. *Nature* **452:** 741–744.

Tripp, H.J., Schwalbach, M.S., Meyer, M.M., Kitner, J.B., Breaker, R.R., and Giovannoni, S.J. (2009) Unique glycine-activated riboswitch linked to glycine-serine auxotrophy in SAR11. *Environ Microbiol* **11:** 230–238.

Vadstein, O. (2000) Heterotrophic, planktonic bacteria and cycling of phosphorus: phosphorus requirements, competitive ability, and food web interactions. *Adv Microb Ecol* **16:** 115–167.

Warren, R.A.J. (1996) Microbial hydrolysis of polysaccharides. *Annu Rev Microbiol* **50:** 183–212.

Wichels, A., Hummert, C., Elbrächter, M., Luckas, B., Schütt, C., and Gerdts, G. (2004) Bacterial diversity in toxic *Alexandrium tamarense* blooms off the Orkney Isles and the Firth of Forth. *Helgoland Mar Res* **58:** 93–103.

Williams, T.J., Long, E., Evans, F., DeMaere, M.Z., Lauro, F.M., Raftery, M.J., *et al*. (2012) A metaproteomic assessment of winter and summer bacterioplankton from Antarctic Peninsula coastal surface waters. *ISME J* **6:** 1883–1900.

Winnen, B., Hvorup, R.N., and Saier, M.H. (2003) The tripartite tricarboxylate transporter (TTT) family. *Res Microbiol* **154:** 457–465.

Yang, C.Y., Li, Y., Zhou, Y.Y., Zheng, W., Tian, Y., and Zheng, T.L. (2012) Bacterial community dynamics during a bloom caused by *Akashiwo sanguinea* in the Xiamen sea area, China. *Harmful Algae* **20:** 132–141.

Zhang, H., Wang, D.Z., Xie, Z.X., Zhang, S.F., Wang, M.H., and Lin, L. (2015) Comparative proteomics reveals highly and differentially expressed proteins in field-collected and laboratory-cultured blooming cells of the diatom *Skeletonema costatum*. *Environ Microbiol* **17:** 3976–3991.

Zhang, W.P., Sun, J., Cao, H.L., Tian, R.M., Cai, L., Ding, W., and Qian, P.Y. (2016) Post-translational modifications are enriched within protein functional groups important to bacterial adaptation within a deep-sea hydrothermal vent environment. *Microbiome* **4:** 49.

Zhang, Y., Gladyshev, V.N., and Richardson, P.M. (2008) Trends in selenium utilization in marine microbial world revealed through the analysis of the global ocean sampling (GOS) project. *PLoS Genet* **4:** e1000095.

Zhao, W.H., Wang, J.T., and Chen, M.M. (2009) Three-dimensional fluorescence characteristics of dissolved organic matter produced by *Prorocentrum donghaiense* Lu. *Chin J Oceanol Limnol* **27:** 564–569.

Zhou, M.J. (2010) Environmental settings and harmful algal blooms in the sea area adjacent to the Changjiang River estuary. *Coast Environ Ecosyst Issues East China Sea* 133–149.

Zhou, M.J., Yan, T., and Zou, J.Z. (2003) Preliminary analysis of the characteristics of red tide areas in Changjiang River estuary and its adjacent sea. *Chin J Appl Ecol* **14:** 1031–1038.

Zhou, Z.X., Yu, R.C., and Zhou, M.J. (2017) Seasonal succession of microalgal blooms from diatoms to dinoflagellates in the East China Sea: A numerical simulation study. *Ecol Model* **360:** 150–162.

Supporting information

Additional Supporting Information may be found in the online version of this article at the publisher's web-site:

Fig. S1. Venn diagram of OTU cluster (a) and protein number (b). Similarities and differences of OTU cluster and protein at both blooming phases were shown in the diagram. That of the OTU cluster and bacterial proteins showed that most bacterioplankton species were similar in the middle- and late-blooming phase with dramatically different protein compositions.

Fig. S2. Shannon index curves of bacterioplankton community in the middle- (black line) and late- (red line) blooming phases of *P. donghaiense*. Shannon index showed that bacterial community diversity in the middle-blooming phase

(about 5.47 at the plateau) was higher than that in the late-blooming phase (about 2.04).

Fig. S3. Functional classification of TBDRs from different bacterial groups in the middle- and late-blooming phases of *P. donghaiense*.

Table S1. The list of all proteins identified in the middle-blooming phase of *P. donghaiense*. 476 high confident proteins were identified in the middle-blooming phase. The protein ID conformed to the serial number of Tara Ocean sequence. Coverage indicated the sequencing cover degree of proteins identified. The function and origin of bacterial proteins identified are shown in the table.

Table S2. The list of all proteins identified in the late-blooming phase of *P. donghaiense*. 955 high confident proteins were identified in the late-blooming phase. The protein ID conformed to the serial number of Tara Ocean sequence. Coverage indicated the sequencing cover degree of proteins identified. The function and origin of bacterial proteins identified are shown in the table.

Table S3. Details of the samples. The sampling information included the sampling time, the latitude and longitude of the sampling station, the depth of water sampled and the size fraction of the bacterial samples.

Table S4. Pearson correlation coefficients between bacterial abundance and environmental parameters. The correlation coefficients for bacterial abundance and environmental parameters were not significant ($P \geq 0.05$ of all parameters).

Table S5. Predicted substrates of TBDRs from different bacterial groups in the middle- and late-blooming phases of *P. donghaiense*.